Comparison of a CCD and an APS for soft X-ray diffraction

2011 JINST 6 C12062

(http://iopscience.iop.org/1748-0221/6/12/C12062)

PUBLISHED BY IOP PUBLISHING FOR SISSA

RECEIVED: *September 13, 2011*
ACCEPTED: *November 25, 2011*
PUBLISHED: *December 22, 2011*

13th INTERNATIONAL WORKSHOP ON RADIATION IMAGING DETECTORS,
3–7 JULY 2011,
ETH ZURICH, SWITZERLAND

2011 JINST 6 C12062

Comparison of a CCD and an APS for soft X-ray diffraction

Graeme Stewart,[a,1] **R. Bates,**[a] **A. Blue,**[a] **A. Clark,**[c] **S. S. Dhesi,**[b] **D. Maneuski,**[a] **J. Marchal,**[b] **P. Steadman,**[b] **N. Tartoni**[b] **and R. Turchetta**[c]

[a] *University of Glasgow, School of Physics and Astronomy, Kelvin Building, University Avenue, Glasgow, G12 8QQ, U.K.*
[b] *Diamond Light Source Ltd, Diamond House, Harwell Science and Innovation Campus, Didcot, Oxfordshire, OX11 0DE, U.K.*
[c] *STFC Rutherford Appleton Laboratory, Harwell Oxford, Didcot, OX11 0QX, U.K.*

E-mail: gd.stewart@physics.gla.ac.uk

[1] Corresponding author.

doi:10.1088/1748-0221/6/12/C12062

ABSTRACT: We compare a new CMOS Active Pixel Sensor (APS) to a Princeton Instruments PIXIS-XO: 2048B Charge Coupled Device (CCD) with soft X-rays tested in a synchrotron beam line at the Diamond Light Source (DLS). Despite CCDs being established in the field of scientific imaging, APS are an innovative technology that offers advantages over CCDs. These include faster readout, higher operational temperature, in-pixel electronics for advanced image processing and reduced manufacturing cost.

The APS employed was the Vanilla sensor designed by the MI3 collaboration and funded by an RCUK Basic technology grant. This sensor has 520 x 520 square pixels, of size 25 μm on each side. The sensor can operate at a full frame readout of up to 20 Hz. The sensor had been back-thinned, to the epitaxial layer. This was the first time that a back-thinned APS had been demonstrated at a beam line at DLS.

In the synchrotron experiment soft X-rays with an energy of approximately 708 eV were used to produce a diffraction pattern from a permalloy sample. The pattern was imaged at a range of integration times with both sensors. The CCD had to be operated at a temperature of -55°C whereas the Vanilla was operated over a temperature range from 20°C to -10°C. We show that the APS detector can operate with frame rates up to two hundred times faster than the CCD, without excessive degradation of image quality. The signal to noise of the APS is shown to be the same as that of the CCD at identical integration times and the response is shown to be linear, with no charge blooming effects.

The experiment has allowed a direct comparison of back thinned APS and CCDs in a real soft x-ray synchrotron experiment.

KEYWORDS: X-ray detectors; Hybrid detectors; Photon detectors for UV, visible and IR photons (solid-state) (PIN diodes, APDs, Si-PMTs, G-APDs, CCDs, EBCCDs, EMCCDs etc)

2011 JINST 6 C12062

Contents

2011 JINST 6 C12062

1 Introduction

Charge Coupled Devices (CCDs) are currently used in the majority of imaging applications due to their low noise and high sensitivity [1]. Complementary Metal-Oxide Semiconductors (CMOS) sensors are an alternative technology [2]. Both technologies use a pixelated, semiconductor substrate. CMOS generally have the advantage of faster frame rate compared to CCDs, but usually suffer from higher read-out noise. In this study we will test the feasibility of using a developmental backthinned CMOS sensor in a soft X-ray synchrotron experiment and compare it to a commercial high-perfomance back-illuminated CCD.

1.1 Charge Coupled Devices

CCDs operate by accumulating charge in each pixel in proportion to the incident photon flux. This charge is then passed sequentially down the column, converted to a voltage and passed off-chip to be read as a digital signal (figure 1). CCDs can suffer from blooming where pixels are overloaded and spread their charge to the neighbouring pixels.

The CCD used in our experiment was a Princeton Instruments PIXIS-XO: 2048B with 2048 by 2048 square pixels, with sides 13.5 µm [3]. The PI PIXIS-XO: 2048B CCD offers very high performance in terms of high dynamic range and very low-noise. It is well suited to soft-X-ray detection and is available on the soft X-ray beamline at the Diamond Light Source [4].

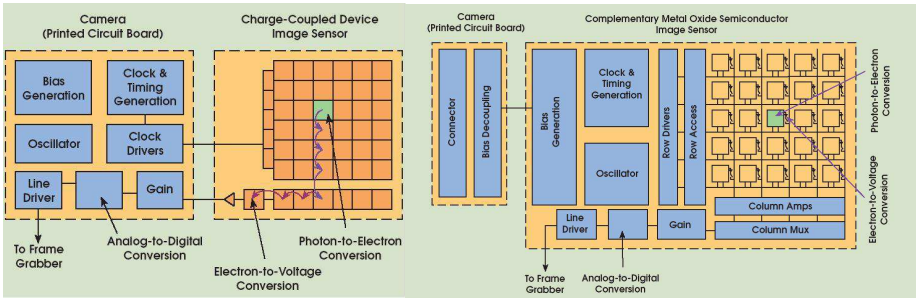

(a) **(b)**

Figure 1. Diagram of generic CCD (a) and CMOS APS (b) layouts [6]. The remainder of the printed circuit board can be customised based on the required specifications.

1.2 Active Pixel Sensors

Active Pixel Sensor (APS) CMOS devices differ from CCDs by including the charge to voltage conversion with each pixel (figure 1). A prototype APS, the Vanilla sensor, was developed by the MI3 collaboration. Each pixel was 25 µm x 25 µm and the maximum frame rate of 20 frames per second was limited by the capacitance load of the wires and the DAQ system. The ability to read out each pixel independently of its neighbours allowed the development of intelligent imaging. The default digital readout employed a 12-bit readout system.

The back thinning was performed by E2V [5]. The process involves removing the substrate below the epitaxial layer of the CMOS sensor. This allows back-illumination of the CMOS sensor and improves signal collection compared to front-illumination, particularly for low energy X-rays. The epitaxial layer of the Vanilla sensor used in this study was 14 µm.

1.3 Noise

There are three main sources of noise in any measurement by an APS sensor (Formula (1.1)). The photon shot noise is proportional to the square root of the incident photon intensity and is caused by a statistical process described by Bose-Einstein statistics [7]. It is related to the charge generated by a photon's interaction with the semiconductor.

$$\sigma^2_{\text{Total}} = K^2(\sigma_d^2 + \sigma_e^2) + \sigma_q^2 \tag{1.1}$$

Formula (1.1): Total Noise as a function of its components. σ_d is the read noise; σ_e is the shot noise; σ_q is the fixed pattern noise [8].

The second class of noise is fixed pattern noise (FPN). This is caused by each pixel on the sensor having different charge collection efficiencies and different amplifier gains and is spatially constant from frame to frame. This noise is proportional to the signal, but can be corrected in post-processing. Any other source of noise is classed as read noise, and is independent of the signal. The total noise is calculated by summing all the previous sources of noise in quadrature.

1.4 Photon Transfer Curve

In a sensor, the incoming signal is measured by the number of electrons it creates in the silicon substrate. This is then converted to Digital Numbers (DN) for reading out. The ratio of electrons

2011 JINST 6 C12062

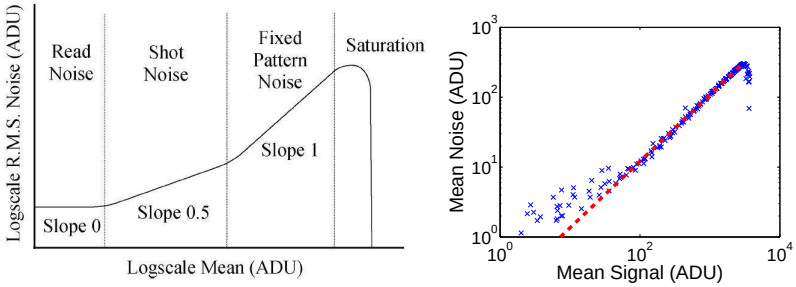

(a) **(b)**

Figure 2. (a) Generic Photon Transfer Curve, showing the four main sections identifiable. (b) The PTC curve for the vanilla sensor in default mode, after pedestal subtraction. The red dashed line gives the fit to the shot noise section of the graph, with the x-intercept being the camera gain.

per DN is the camera's gain. One method for measuring this gain is the Photon Transfer Curve (PTC) (figure 2a) [9]. The detector was illuminated uniformly with visible light, using an LED set up in a dark box. The noise level is measured by taking the standard deviation of a series of images once the pedestal has been subtracted, removing the FPN.

The PTC allows several aspects of the detector to be analysed. The full well capacity is given by the signal before saturation. The dynamic range is the range over which shot noise and fixed pattern noise is dominant. The gain is given by the slope of the shot-noise region of the PTC curve. In log-log scale, this value is obtained by fitting the shot-noise region of the PTC curve with a straight line and finding the ADU value corresponding to the intersection point with the x-axis. The APS gain was found to be 7.25 e^-/DN, the full well capacity was 2200 e^- and the dynamic range was approximately 20 000 e^- (figure 2b).

2 Results

In order to compare the CCD and APS sensors, a standard experiment was selected. Beamline I06 was chosen to use soft x-rays, at an energy of 708 eV, to create a diffraction pattern from a permalloy sample (figure 3). This is typical of a soft X-ray experiment [4].

2.1 CCD and APS signals with varying frame rates

Both the APS and CCD were used to take images at a variety of frame rates with integration times varying between 10 seconds and 5 minutes for the CCD, and between 0.05 seconds and 10 seconds for the APS. From these images, a simple line profile through the diffraction spots can be used to derive the peak to trough ratio (figures 4 and 5). For the CCD, the peak to trough varied between 10^2 - 10^4 whereas the Vanilla sensor varied between 10^1 - 10^3. Blooming is observed in the CCD at the longest integration times.

2.2 Dark current

In any photosensitive device, a small current will be present even when there are no incident photons due to the random creation of thermal electron hole pairs in the depletion region. This dark

2011 JINST 6 C12062

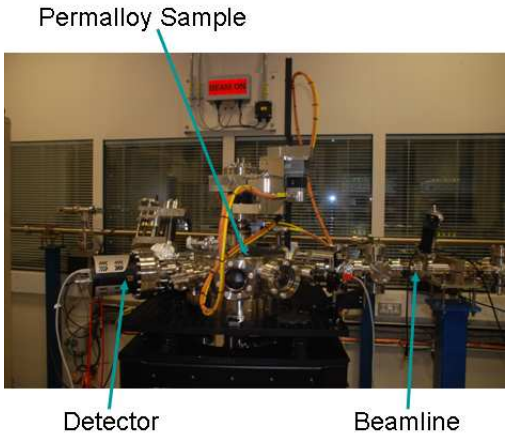

Figure 3. Schematic of experimental set up, showing beam, sample and detector.

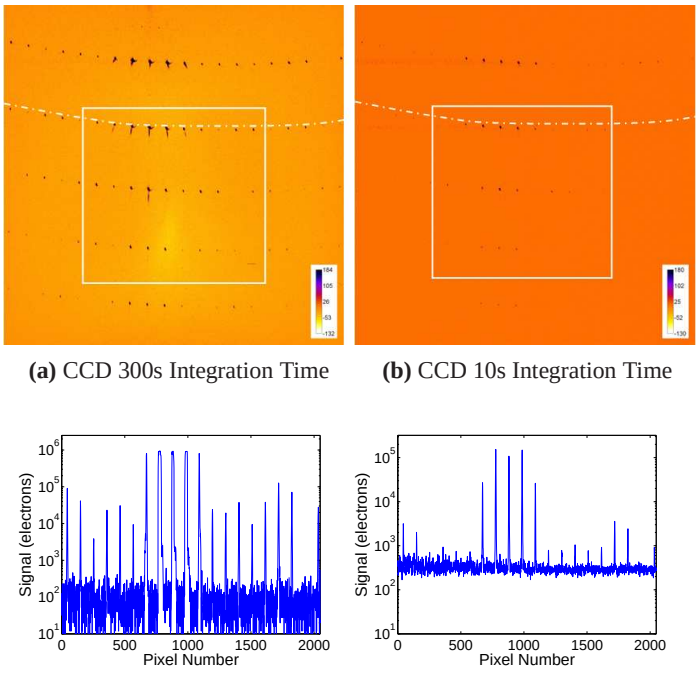

(a) CCD 300s Integration Time **(b)** CCD 10s Integration Time

Figure 4. CCD images and line profiles from (a) the longest integration time (300s) and (b) the shortest integration time (10s). Images have had pedestals subtracted. The line profile consists of the summation of three adjacent pixels along the dotted line. The square indicates the region imaged by the Vanilla sensor.

current has fixed and shot noise components. The CCD used showed significantly less dark current (2 x 10^{-9} $e^{-}\mu m^{-2}s^{-1}$ at -55°C) than the APS (4 x 10^{-7} $e^{-}\mu m^{-2}s^{-1}$ at -10°C)(figure 6). The dark current in silicon should half every 7°C, so between 20°C and -55°C there should be a reduction by three orders of magnitude.

2011 JINST 6 C12062

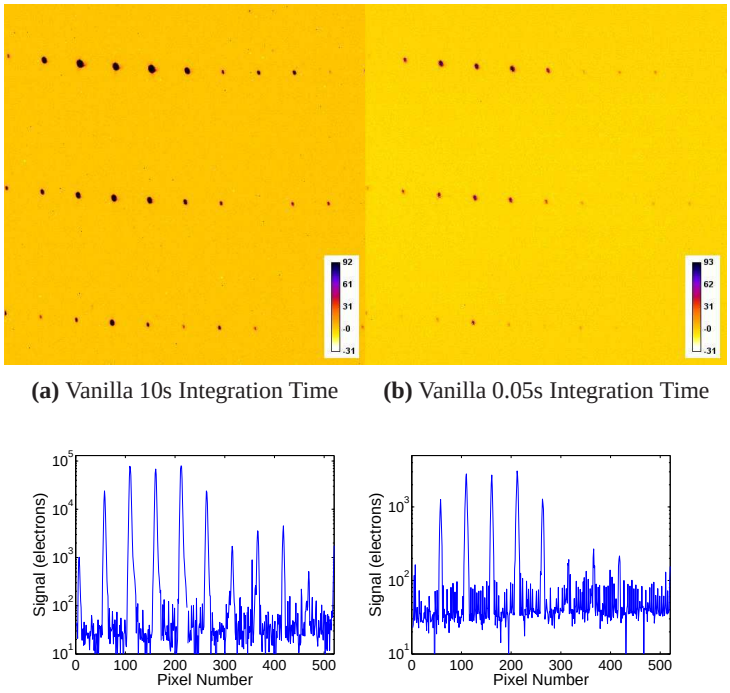

(a) Vanilla 10s Integration Time **(b)** Vanilla 0.05s Integration Time

Figure 5. Vanilla images and line profiles from (a) the longest integration time (10s) and (b) the shortest integration time (0.05s). Images have had pedestals subtracted. The area covered by the Vanilla is a quarter of that covered by the CCD.

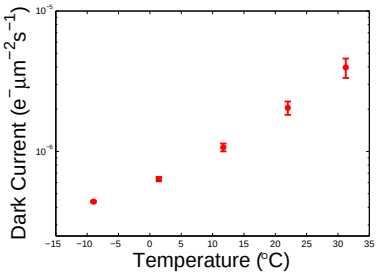

Figure 6. Dark current against temperature for the Vanilla CMOPS APS. Vanilla reached a dark current of 10^{-6} $e^{-}\mu m^{-2}s^{-1}$ at -20°C, and the CCD dark current was 2 x 10^{-9} $e^{-}\mu m^{-2}s^{-1}$ at -55°C.

2.3 Noise measurements

In order to quantify the noise, a series of dark images were recorded at different temperatures. From these, the average pedestal signal was subtracted and the variance of the resultant image gives the read noise (figure 7). At -55°C, the CCD's two operational modes, low noise and high capacity, each have different noise levels. The low noise mode has a noise level of around 20 electrons, whereas the high capacity mode has a level of around 50 electrons. The Vanilla sensor's noise was around 20 electrons, increasing to 35 electrons at the longest integration time.

2011 JINST 6 C12062

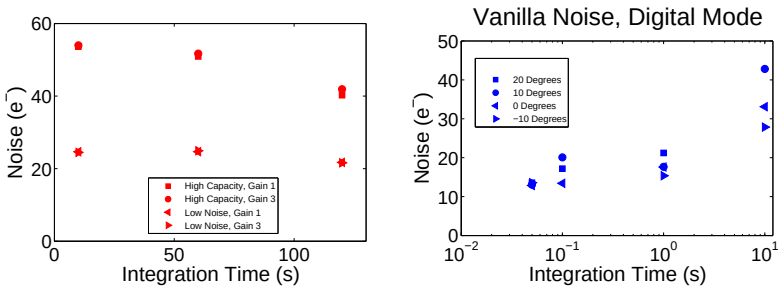

Figure 7. Noise levels for (a) the CCD and (b) the Vanilla sensor.

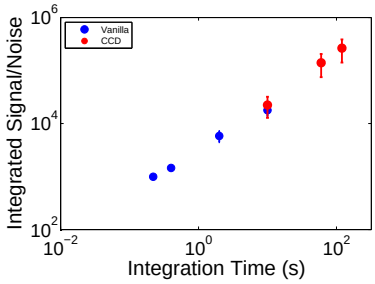

Figure 8. Signal to Noise ratio for the CCD and Vanilla.

2.4 Signal to noise analysis

The method used to measure the signal to noise ratio was to sum the charge from a spot, and then compare this with the baseline noise level (figure 8). The brightest spot from the second order diffraction was chosen, to prevent saturation affecting the result. The total charge collected increased linearly with integration time, with the CCD increasing from 10^4 to 10^6 and Vanilla increasing from 2 x 10^2 to 10^4 with an agreement, within error, at the same integration rate.

Whilst a quantitative measurement of the efficiency of each sensor was not possible, a comparison was performed. For the equivalent diffraction spot in both the CCD and Vanilla sensors, 8 x $10^4 \pm 2$ x $10^4 e^-/s$ were collected regardless of integration time. From this we can deduce that the efficiencies of the two sensors were comparable.

3 Conclusions

The Vanilla sensor, despite not being designed specifically for the experiment performed, showed competitive results to the leading CCD sensor (table 1). The frame rate of the Vanilla was two hundred times greater than the CCD with full frame readout. At -55°C, the read noise in the CCD was stable at $20e^-$ or $50e^-$ depending on the collection mode. The read noise in Vanilla was between $15e^-$ and $35e^-$ depending on the operating temperature. The signal to noise ratio was comparable between CCD and CMOS APS at identical integration times. There are applications where an APS sensor could out-perform a traditional CCD.

2011 JINST 6 C12062

Table 1. Comparison of the key characteristics of the CCD and Vanilla sensors.

	Maximum Frame Rate	Operating Temperature	Read Noise	Peak to Trough	Signal to Noise
Princeton PIXIS CCD	0.1fps	-55°C	$20e^-$ - $50e^-$	10^2 - 10^4	10^4 - 10^6
Vanilla CMOS APS	20fps	-10°C	$15e^-$ - $120e^-$	10^1 - 10^3	10^3 - 10^4

Acknowledgments

We thank Brian Willis and Damien Barnett from the Detector Group of the Diamond Light Source for their assistance in developing the in-vacuum Vanilla CMOS sensor set-up used for this study.

References

[1] P. Magnan, *Detection of visible photons in CCD and CMOS: a comparative view*, *Nucl. Instrum. Meth.* **A 504** (2003) 199.

[2] A. Blue et al., *Characterisation of Vanilla: a novel active pixel sensor for radiation detection*, *Nucl. Instrum. Meth.* **A 581** (2007) 287.

[3] *PIXIS-XO:* 2048*B*, http://www.infim.ro/∼lab180/projects/2007/PNCD2/PN2C/MICROREXMOS/Princeton_Instruments_PIXIS_XO_2048B_RevB0.pdf, (2010).

[4] S.S. Dhesi et al., *The nanoscience beamline (I*06*) at diamond light source*, in 10th *International conference on radiation instrumentation*, *AIP Conf. Proc.* **1234** (2010) 311.

[5] P. Jerram et al., *Back-thinned CMOS sensor optimization*, in *Optical Components and Materials VII*, *Proc. SPIE Int. Soc. Opt. Eng.* **7598** (2010) 759813.

[6] D. Litwiller, *CCD vs. CMoS: facts and fiction*, http://www.dalsa.com/public/corp/photonics_spectra_ccdvscmos_litwiller.pdf, Waterloo Canada (2001).

[7] J.R. Janesick, *Photon transfer*, SPIE Press, Bellingham U.S.A. (2007).

[8] European Machine Vision Association, *EMVA Standard* 1288*: standard for characterization of image sensors and cameras*, http://www.emva.org/cms/upload/Standards/Stadard_1288/EMVA1288-3.0.pdf, (2010).

[9] S.E. Bohndiek et al., *Comparison of methods for estimating the conversion gain of CMOS active pixel sensors*, *IEEE Sensors J.* **8** (2008) 1734.

2011 JINST 6 C12062